Fruit Research

ARTICLE

Open Access

https://doi.org/10.48130/frures-0026-0037

Fruit Research **2026**, 6: e043

Insights into the nutritional quality formation of Zhaotong apples revealed by electronic sensory and metabolomic analyses

Xin Li[1], Ming Zhang[1*], Yuheng Xiang[1], Yulong Li[1], Xiao Ma[2] and Kunyi Liu[3]

[1] *College of Biological Science and Food Engineering, Forest Resources Exploitation and Utilization Engineering Research Center for Grand Health of Yunnan Provincial Universities, Southwest Forestry University, Kunming 650224, China*

[2] *College of Food Science and Technology, Yunnan Agricultural University, Kunming 650201, China*

[3] *School of Wuliangye Technology and Food Engineering, Yibin Vocational and Technical College, Yibin 644100, China*

* Correspondence: 18445863960@163.com (Zhang M)

Abstract

This study investigated four apple cultivars—Golden Venus (VG), Ruixue (RX), Ruixianghong (RXH), and Red Fuji (RFJ)—grown in the low-latitude, high-altitude ecology of Zhaotong, analyzing their phenotypic, nutritional, and flavor characteristics alongside untargeted metabolomics. Results showed RFJ had the largest fruit size and weight, while VG, RX, and RXH excelled in total sugars and total soluble solids (TSS). In functional quality, RXH displayed the highest total polyphenols, anthocyanins, and antioxidant activity, whereas VG was richest in vitamins C and E. Electronic sensory analysis (e-nose and e-tongue) revealed predominantly fresh and sweet taste profiles across all cultivars, with RX releasing significantly stronger sulfide-related volatile compounds. Metabolomic profiling demonstrated sharp inter-cultivar differentiation driven by carbohydrate and amino acid pathways, with the pentose phosphate pathway most significantly enriched. Correlation analysis revealed a potential trade-off between key quality indices—such as TSS and soluble sugars—and free amino acids (e.g., L-isoleucine). Concurrently, electronic sensory attributes (acidity, bitterness/astringency) were closely associated with the dynamic changes in primary metabolites, including polysaccharides and free amino acids. Overall, this study elucidates the metabolic regulatory mechanisms governing flavor and quality formation in Zhaotong apples, providing a scientific basis for regional cultivar improvement.

Keywords: Apple, Nutritional quality, Electronic tongue, Electronic nose, Metabolomics

Citation: Li X, Zhang M, Xiang Y, Li Y, Ma X, et al. 2026. Insights into the nutritional quality formation of Zhaotong apples revealed by electronic sensory and metabolomic analyses. *Fruit Research* 6: e043 https://doi.org/10.48130/frures-0026-0037

Introduction

Apple (*Malus domestica* Borkh.), a member of the genus *Malus* within the family Rosaceae, ranks among the four major cultivated fruits globally[1]. As the prominent global leader in pomology, China continuously drives international apple production, accounting for over half of the global annual yield and firmly maintaining its top rank worldwide[2]. Zhaotong apple production represents one of the most critical pillar industries driving the agricultural economy and rural revitalization in Zhaotong City, China[3]. Owing to the unique geographical advantages of low latitude and high altitude, coupled with abundant sunlight and significant diurnal temperature variations, Zhaotong apples exhibit high soluble solids content, a crisp and fine flesh texture, and a rich flavor profile. These distinctive attributes endow them with strong market competitiveness and high consumer preference.

However, the Zhaotong apple industry currently suffers from an imbalanced varietal structure characterized by a prominent lack of diversity. Mid-to-late maturing varieties, dominated by 'Red Fuji', account for over 65% of the total production, whereas early- and mid-maturing varieties are severely deficient. With shifting consumer demands for enhanced apple quality and varietal diversity, alongside intensifying industrial competition, the existing varietal structure dominated by mid-to-late maturing 'Red Fuji' can no longer satisfy market requirements. In recent years, mid-maturing apple cultivars such as 'Venus Gold', 'Ruixue', and 'Ruixianghong' have emerged as prime candidates for structural adjustment in Zhaotong due to their optimal ripening periods, superior quality, and high market value. Nevertheless, driven by the pursuit of high economic returns from mid-maturing varieties, growers often introduce these cultivars blindly. Poor regional adaptability and uncharacterized nutritional profiles risk introduction failure and economic loss. Consequently, this study comprehensively evaluates introduced mid-maturing apple cultivars in Zhaotong to establish rigorous selection and quality criteria. Nutritional quality dictates market competitiveness and germplasm utilization. Beyond conventional indices (sugars, organic acids, vitamin C, soluble solids) and mineral profiling (potassium, calcium, magnesium, micronutrients) that reflect foundational value, integrating advanced analytical techniques and electronic sensory evaluation provides objective, multi-dimensional assessment frameworks for cultivar screening[4–6]. Furthermore, objective evaluation and recognition methods powered by electronic sensory systems, such as electronic noses and electronic tongues, enable the objective, rapid, and non-destructive assessment of fruit traits[7,8]. Concurrently, widely targeted metabolomics based on ultra-high-performance liquid chromatography-quadrupole time-of-flight mass spectrometry (UPLC-Q-TOF-MS) or gas chromatography-mass spectrometry (GC-MS) allows for the systematic elucidation of the molecular mechanisms underlying fruit quality formation at the metabolite level. This facilitates the screening of differential metabolic markers, thereby providing a deeper scientific foundation for quality evaluation[9,10]. These methodologies have been systematically applied to evaluate fruit quality across various fruit trees, including goji berry, kiwifruit, grape, mango, and citrus[11–15]. However, existing studies have predominantly focused on single quality traits or conventional nutritional component analysis; comprehensive evaluations of mid-maturing apple cultivars integrated with multi-omics data remain

© The Author(s)

https://doi.org/10.48130/frures-0026-0037

scarce. Currently, there is a lack of systematic research comparing the nutritional variations among the introduced cultivars 'Venus Gold', 'Ruixue', and 'Ruixianghong' and the primary cultivated variety 'Red Fuji' in the Zhaotong region. Crucially, a comprehensive evaluation framework bridging nutritional quality, mineral elements, sensory attributes, and widely targeted metabolomics has not yet been established. This deficiency in scientific and standardized nutritional evaluation criteria and screening methodologies heavily constrains the evidence-based introduction and promotion of mid-maturing cultivars in Zhaotong.

In this study, the mid-maturing apple cultivars 'Venus Gold', 'Ruixue', and 'Ruixianghong' introduced and cultivated in the Zhaotong region, alongside the primary late-maturing cultivar 'Red Fuji', were selected as the research subjects. A multi-dimensional analytical approach was deployed to systematically evaluate the core quality traits of these different apple cultivars. This approach encompassed nutritional quality indices (soluble sugars, total acidity, sugar-acid ratio, vitamin C, soluble protein, and soluble solids content), mineral elements (potassium, calcium, magnesium, iron, zinc, and selenium), electronic sensory evaluations via electronic nose and electronic tongue, and untargeted metabolomic characterization. To construct a comprehensive nutritional quality evaluation framework for mid-maturing apples, descriptive statistical analysis, principal component analysis (PCA), hierarchical cluster analysis (HCA), orthogonal partial least squares-discriminant analysis (OPLS-DA), and Kyoto Encyclopedia of Genes and Genomes (KEGG) pathway enrichment analysis were employed. This study aims to clarify the variations in fruit nutritional quality performance among apple cultivars with different ripening periods under the unique low-latitude and high-altitude climate conditions of Zhaotong. Furthermore, it seeks to identify key differential metabolites and metabolic pathways that characterize mid-maturing varieties, and establish a multi-omics data-driven nutritional quality evaluation model. Ultimately, these findings will provide a solid theoretical foundation and technical support for structural adjustments of apple varieties, the scientific promotion of mid-maturing cultivars, and the high-quality development and utilization of germplasm resources in Zhaotong.

Materials and methods

Experimental materials

Plant materials: Four economically significant apple cultivars (*Malus domestica*) grown in Zhaotong City, Yunnan Province, China—namely 'Golden Venus' (VG), 'Ruixue' (RX), 'Ruixianghong' (RXH), and 'Red Fuji' (RFJ)—were selected as experimental materials. Fruit were harvested in mid-October from a standardized demonstration orchard in Zhaotong's core production belt (27°20' N, 103°42' E; altitude 1,950 m a.s.l.). All test trees were 6-year-old scions grafted onto *Malus robusta* Rehd. rootstocks, trained to a slender spindle architecture at a spacing of 1.5 m × 4 m, and managed under uniform horticultural conditions, including drip irrigation, localized fertigation, and integrated pest management. Commercial harvest maturity across cultivars was strictly standardized using the Cornell starch–iodine index (scale 1–8, target 5.0–6.0), fruit firmness (6.5–7.5 kg/cm^2 via FT-327 penetrometer), and characteristic background skin coloration. Sampling followed a randomized complete block design: for each cultivar, 30 uniform, defect-free fruits were hand-harvested from the outer and middle canopies of 10 representative trees (three fruit per tree) and transported to the laboratory at 4 °C within 2 h. After non-destructive physical evaluations, equatorial mesocarp tissues were quickly excised—excluding the ~1 mm peel and core carpel tissue—pooled, flash-frozen in liquid nitrogen, and stored at −80 °C until analysis; six and five independent biological replicates were prepared for metabolomic profiling and physicochemical determinations, respectively, with each replicate derived from a homogenized pool of five to six fruit.

Phenotypic measurement

Extrinsic quality measurement: The mass of a single fruit (fruit, FW) is measured using a Mettler electronic balance MA204E. The longitudinal diameter (LD) and transverse diameter (TD) of the fruit are measured using a digital vernier caliper, with the maximum and minimum values recorded.

Internal quality indicators

Determination of total soluble solids content (TSS)

Five grams of apple pulp were taken, and 25 mL of deionized water was added to extract juice. The mixture was centrifuged at 4 °C and 12,000 r/min for 10 min, and the supernatant was collected. A handheld digital refractometer was used to measure the total soluble solids (TSS) content of the sample. This process was repeated three times for each sample, and the average value was taken. The result is expressed as a %[16].

Determination of total soluble sugar content

A 1.0 g sample of apple homogenate was taken, and 5.0 mL of deionized water, 200 μL of 15% $K_4(Fe[CN]_6)$, and 200 μL of 30% $ZnSO_4$ were added, then sealed with a double-layer sealing film, vortexed for 5 min, centrifuged at 10,000 r/min at low temperature for 15 min, and the supernatant was taken. The filtrate was diluted with ultrapure water 10 times, and 5.0 μL was taken for injection. The chromatographic column is an Asahipak NH_2P-50 (250 mm × 4.6 mm, 5 μm), the column temperature is 30 °C, and an evaporative light scattering detector is used. The mobile phase consisted of water (phase A) and acetonitrile (phase B) (1:3, v/v) under isocratic elution at a flow rate of 1.0 mL/min. Quantification of sorbitol, sucrose, glucose, and fructose was performed using the external standard method with mixed reference standards, and each sample was analyzed in triplicate[17].

Determination of total acidity (TA)

A 5.0 g sample of apple homogenate was weighed and diluted to a final volume of 50 mL using deionized water. The mixture was then titrated to a fixed endpoint of pH 8.1 with a 0.1 mol/L sodium hydroxide standard solution using an automatic potentiometric titrator, and the total volume of the consumed sodium hydroxide solution was recorded. The final titratable acidity content was determined based on the volume of sodium hydroxide consumed, its molar concentration, the initial sample mass, and the specific conversion factor for malic acid, with the final value expressed as malic acid equivalent[18].

Determination of total dietary fiber (TDF) content

A 1.0 g sample of apple homogenate was weighed and mixed with 50 mL of MES-TRIS buffer. Enzymatic hydrolysis was sequentially performed by adding α-amylase (at 95 °C for 35 min), protease (at 60 °C for 30 min), and amyloglucosidase (at 60 °C for 30 min). The mixture was then precipitated with four volumes of 95% ethanol and filtered to collect the residue. The obtained residue was washed sequentially with 78% ethanol, 95% ethanol, and acetone, followed

by drying at 105 °C until a constant weight was achieved. After correcting for protein and ash contents determined from the residue, the total dietary fiber content was expressed as g/100 g on a dry weight basis[19].

Determination of soluble pectin (SP) content

A 5.0 g sample of apple homogenate was weighed, mixed with 50 mL of distilled water preheated to 70 °C, and stirred continuously for 1 h to extract soluble pectin. The mixture was then centrifuged, and the supernatant was collected and diluted to a final volume of 100 mL. A 1 mL aliquot of the extract was transferred to a tube, and 6 mL of concentrated sulfuric acid was added under an ice-water bath. After thorough mixing, 0.2 mL of a 0.15% carbazole-absolute ethanol solution was added, and the mixture was homogenized completely. The mixture was allowed to stand at room temperature for 2 h, after which the absorbance was measured at a wavelength of 530 nm. The soluble pectin content was quantified using a standard curve generated with D-galacturonic acid, and the final results were expressed as g/100 g[20].

Nutritional quality parameters

Determination of total phenolic content (TPC)

A 1.0 g sample of apple homogenate was accurately weighed into a centrifuge tube, mixed with an appropriate volume (10–20 mL) of an 80% methanol (or ethanol) solution, and subjected to ultrasonic extraction for 30 min under dark conditions. The mixture was then centrifuged at 8,000 rpm for 10 min to collect the supernatant. The remaining residue was re-extracted once following the same procedure, and the combined supernatants were precisely diluted to a final volume of 25 mL in a volumetric flask with the extraction solvent to serve as the sample extract. For the colorimetric reaction, a 1.0 mL aliquot of the sample extract was transferred to a test tube, followed by the sequential addition of 1.0 mL of Folin–Ciocalteu reagent and 2.0 mL of a 7.5% (w/v) sodium carbonate (Na_2CO_3) solution. The mixture was diluted to a constant volume with distilled water, thoroughly homogenized, and allowed to react in a water bath at 30 °C for 1 h in the dark to form a stable blue complex. Finally, the absorbance of the reaction mixture was measured at 765 nm using a spectrophotometer. The total phenolic content was quantified against a simultaneously prepared gallic acid standard calibration curve and expressed per gram of apple sample[21,22].

Determination of total anthocyanin content (TAC)

Apple peel or pulp powder (1.0 g) was mixed with 20 mL of a 1% HCl-methanol solution and extracted at 4 °C in the dark for 24 h. The mixture was centrifuged at 8,000 r/min for 10 min, and the supernatant was collected and diluted to 25 mL. A 1 mL aliquot of this extract was diluted to a final volume of 10 mL using a pH 1.0 potassium chloride buffer (0.025 mol/L), and another 1 mL aliquot was similarly diluted to 10 mL using a pH 4.5 sodium acetate buffer (0.4 mol/L). After equilibration at room temperature for 15 min, the absorbance of both dilutions was measured at 510 and 700 nm using the respective buffers as blanks. The total anthocyanin content was determined using the pH differential method and calculated as cyanidin-3-O-glucoside equivalents (mg/100 g). Each sample was analyzed in triplicate[23].

Determination of vitamin C (VC) content

A 1.0 g sample of apple puree was homogenized with 4.0 g of an extraction buffer (pH 2.0) containing 10.0 g/L metaphosphoric acid and 5.0 g/L oxalic acid, and vortexed thoroughly to ensure complete dispersion. The mixture was centrifuged at 10,000 × *g* for 30 min at 4 °C, and the supernatant was collected as the crude vitamin C extract. To prepare the total vitamin C analytical solution, a phosphate buffer containing 2.5 mmol/L TCEP was added to the extract to adjust the system pH to 3.5; the mixture was homogenized, centrifuged at 10,000 × *g* for 15 min at 4 °C, and filtered through a 0.45 μm organic phase membrane filter. To prepare the reduced ascorbic acid analytical solution, a 0.1 mol/L phosphate buffer (pH 2.0) was added to the extract to adjust the pH to 3.5, processed under identical centrifugation conditions for 15 min, and filtered through a 0.45 μm membrane filter. For chromatographic analysis and quantification, a 25 μL aliquot of each analytical solution was injected into a reversed-phase high-performance liquid chromatography (RP-HPLC) system. Separation was performed on a TC-C_{18} (250 mm × 4.6 mm, 5 μm) utilizing a mobile phase consisting of a mixed solution containing 1.0 mmol/L EDTA and 10.0 mmol/L CH_3COONH_4 (pH 3.0) at a flow rate of 0.8 mL/min, with UV detection at 245 nm. Absolute quantification was achieved using an external standard curve established with an ascorbic acid standard[24].

Determination of vitamin E (VE) content

A 1.0 g sample of apple puree was mixed with absolute ethanol and the antioxidant butylated hydroxytoluene (BHT), and subsequently subjected to ultrasonic extraction using n-hexane. The collected organic phase was washed until neutral, dehydrated with anhydrous sodium sulfate, and concentrated to dryness under a low-temperature nitrogen stream or via rotary evaporation. The resulting residue was reconstituted in a chromatographic-grade solvent and filtered through a 0.22 μm microfiltration membrane for subsequent analysis. Chromatographic separation was conducted on a C18 reversed-phase column utilizing a methanol-water mobile phase system. Detection was achieved using a fluorescence detector (excitation wavelength: 294 nm, emission wavelength: 328 nm). Vitamin E was qualitatively identified based on retention time and precisely quantified using the external standard method based on peak area calibration curves[25].

Evaluation of antioxidant activities

ABTS radical scavenging activity assay

A 20 μL aliquot of the diluted apple homogenate was added to a 96-well plate, followed by the sequential addition of 160 μL of phosphate buffer (pH 7.2) and 40 μL of a stable $ABTS^+$ working solution. The working solution was prepared by reacting 7 mM ABTS with 2.45 mM potassium persulfate in the dark for 16 h and subsequently diluting the mixture with ethanol to achieve an absorbance at 734 nm. After incubation at room temperature in the dark for 15 min, the absorbance was measured at 734 nm. The phosphate buffer was used as the blank control, and the radical scavenging rate was calculated accordingly[26].

DPPH radical scavenging activity and Ferric Reducing Antioxidant Power (FRAP) assays

For the DPPH assay, a 20 μL aliquot of the diluted apple sample was mixed with 160 μL of phosphate buffer (pH 7.2) and 40 μL of a 0.2 mM DPPH-ethanol solution. Following a 15 min reaction period at room temperature in the dark, the absorbance was measured at 517 nm. A mixture of the buffer and DPPH solution served as the blank control, with ascorbic acid utilized as the positive control to determine the scavenging rate and the half-maximal inhibitory concentration IC_{50} value[27].

https://doi.org/10.48130/frures-0026-0037

Electronic nose (e-nose) analysis

A 10 g portion of apple pulp collected from the equatorial mesocarp was finely chopped and rapidly sealed into a 50 mL headspace vial, followed by equilibration at room temperature (25 ± 1 °C) for 30 min to enrich headspace volatile organic compounds. Volatile aroma profiling was conducted using a PEN3 portable electronic nose system (Airsense Analytics GmbH, Schwerin, Germany) equipped with an array of 10 metal oxide semiconductor (MOS) sensors (W1C, aromatic compounds; W5S, nitrogen oxides; W3C, ammonia and aromatic components; W6S, hydrogen; W5C, alkanes and aromatic components; W1S, broad-methane; W1W, sulfur compounds; W2S, broad-alcohols; W2W, aromatic and sulfur-containing compounds; and W3S, methane-aliphatics). Zero-grade dry air filtered through activated charcoal was used as the carrier gas at a constant flow rate of 150 mL/min to flush the system (120 s) and establish a stable baseline (zeroing time: 10 s) prior to each measurement. The operational parameters were configured with a pre-sampling time of 5 s, a sampling interval of 1 s, and a total continuous detection time of 120 s. The feature response value for each sensor was extracted as the average relative conductivity (G/G_0, where G and G_0 represent the sensor conductivity in the sample headspace gas and reference clean air, respectively) during the steady-state response plateau between 100 and 115 s. The resulting feature datasets were zero-centered, normalized, and compiled into data matrices for radar chart visualization and downstream multivariate chemometric analyses (n = 5 independent biological replicates)[28].

Electronic tongue (e-tongue) analysis

A 20 g sample of apple pulp was mixed with 100 mL of ultrapure water, homogenized in an ice-water bath, and extracted at 4 °C for 30 min. The mixture was centrifuged at 8,000 × g for 10 min, and the supernatant was filtered through a 0.45 μm microfiltration membrane to yield the liquid sample extract. Taste profile evaluation was conducted using an SA402B electronic tongue system (Insent Inc., Atsugi-shi, Japan) equipped with five lipid membrane potentiometric taste sensors—sourness (CA0), bitterness (C00), astringency (AE1), umami (AAE), and saltiness (CT0)—as well as three secondary sensors monitoring aftertastes (aftertaste-A: astringency aftertaste; aftertaste-B: bitterness aftertaste; richness: umami aftertaste). Prior to measurement, the sensor array was calibrated in a standard reference solution (30 mM KCl and 0.3 mM tartaric acid) until resting potentials reached equilibrium. An 80 mL aliquot of the filtrate was placed into a specialized sample cup. The sensors were sequentially immersed into the sample solution, with data acquisition sustained for 120 s per sample. The stable potentiometric membrane potential output (mV) recorded at 120 s relative to the reference solution baseline was extracted as the characteristic feature score for each taste attribute. Between successive sample runs, sensors underwent a two-step cleaning protocol, and potential sensor drift and response repeatability were evaluated prior to multivariate chemometric analysis (n = 5)[29].

Untargeted metabolomics (UPLC-MS/MS) analysis

Sample preparation: Apple flesh stored at −80 °C was ground under liquid nitrogen, and a 100 mg aliquot was extracted with 1.0 mL of pre-cooled methanol/water (4:1, v/v) containing 10 μg/mL 2-chloro-L-phenylalanine as an internal standard. Following vortexing (1 min), ultrasonic extraction (4 °C, 30 min), protein precipitation (−20 °C, 1 h), and centrifugation (12,000 × g, 15 min, 4 °C), the supernatants were filtered through 0.22 μm PTFE membranes (n = 6 biological replicates per cultivar). Equal aliquots (20 μL) from each sample were pooled to generate quality control (QC) samples, which were injected every six runs throughout the sequence to ensure system stability and repeatability (RSD of internal standard peak area < 5.0%). Chromatographic separation was conducted on an ACQUITY UPLC HSS T3 column (100 mm × 2.1 mm, 1.8 μm; Waters Corp.) at 40 °C with a flow rate of 0.4 mL/min and an injection volume of 4 μL, utilizing a gradient mobile phase of 0.1% formic acid in water (A) and acetonitrile (B) (0–2 min, 5% B; 2–25 min, 5%–95% B; 25–27 min, 95% B; 27–28 min, 95%–5% B; 28–30 min, 5% B). Mass spectrometry was executed on a high-resolution Q-TOF-MS system operating in both ESI+ (3.0 kV) and ESI− (2.5 kV) modes across m/z 50–1,200 via data-dependent acquisition (DDA; collision energy: 20–45 eV). Raw data were preprocessed in Progenesis QI (v3.0, Waters) for automated baseline correction, peak alignment, and normalization. Metabolite identification strictly complied with Metabolomics Standards Initiative (MSI) Level 2 criteria: precursor mass tolerance was constrained within $< 5 \times 10^{-6}$, and experimental MS/MS fragmentation patterns were matched against HMDB, METLIN, and MassBank with a spectral similarity score threshold > 70%. Differentially accumulated metabolites (DAMs) were screened based on orthogonal partial least squares discriminant analysis (OPLS-DA) and univariate testing using the combined criteria of variable importance in projection (VIP) > 1.0, fold change (FC) ≥ 1.5 or ≤ 0.67, and false discovery rate (FDR)-adjusted $p < 0.05$[30].

Statistical analysis

Agronomic, physicochemical, and functional quality parameters are presented as mean ± SEM. Differences among the four cultivars were evaluated by one-way analysis of variance (ANOVA) followed by Tukey's HSD post-hoc test. For untargeted metabolomics, data matrices were Pareto-scaled prior to multivariate chemometrics. Principal component analysis (PCA) and orthogonal partial least squares-discriminant analysis (OPLS-DA) were performed using the ropls package in R (v4.2.1). Model robustness and overfitting were evaluated by 7-fold cross-validation and rigorous 200-iteration permutation tests (R^2Y and Q^2 intercepts). Univariate significance testing for metabolites was executed using two-tailed Student's t-tests, with false discovery rates (FDR) controlled via the Benjamini–Hochberg procedure ($q < 0.05$). KEGG metabolic pathway topology and hypergeometric enrichment analyses were conducted using MetaboAnalyst 5.0. Pairwise associations between quality traits, electronic sensor parameters, and differential metabolites were computed using Pearson's correlation coefficient (r) with the R package corrplot.

Results

Evaluation of fruit phenotypic and physical characteristics

The fruit appearance quality traits of four apple cultivars—namely, VG, RX, RXH, and RFJ—cultivated in the Zhaotong region were systematically evaluated (Fig. 1a). Statistical analysis of the fruit longitudinal diameter, transverse diameter, and single-fruit weight revealed no significant differences in any of these parameters among the three mid-maturing cultivars (VG, RX, and RXH). In contrast, the transverse diameter of the RFJ cultivar was significantly larger than that of the other three varieties, reaching an average of 8.26 cm and demonstrating a distinctly larger fruit size profile.

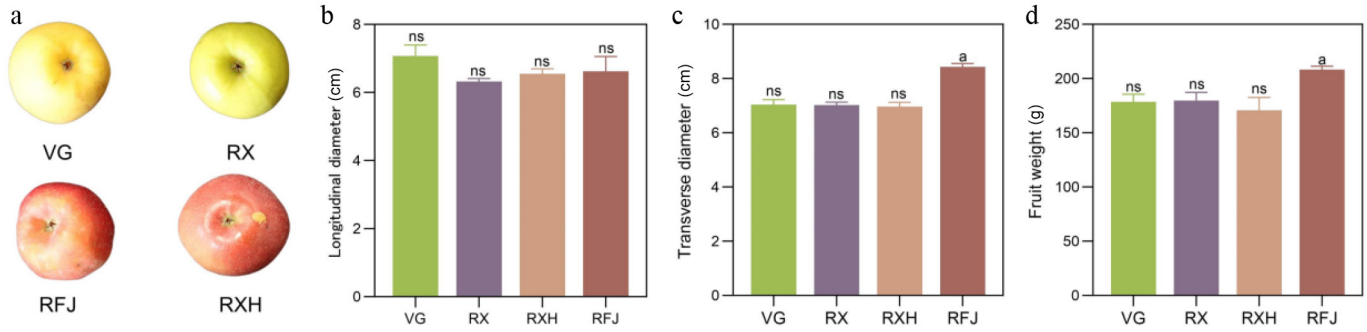


Fig. 1 Comparison of fruit phenotypic and physical characteristics among four apple cultivars. (a) Representative photographs of 'Golden Venus' (VG), 'Ruixue' (RX), 'Ruixianghong' (RXH), and 'Red Fuji' (RFJ) apple fruit grown in Zhaotong. Statistical comparisons of fruit (b) longitudinal diameter, (c) transverse diameter, and (d) single-fruit weight. Data represent mean ± SEM (n = 5). Different lowercase letters indicate statistically significant differences among cultivars according to one-way ANOVA with Tukey's HSD test ($p < 0.05$).

However, no statistically significant differences were observed in the longitudinal diameter among all four cultivars. This indicates that the larger size of 'Red Fuji' fruit is primarily driven by lateral development, resulting in a more robust and oblate overall fruit shape (Fig. 1b, c). Similarly, while the single-fruit weight showed no significant variation among VG, RX, and RXH, that of the RFJ cultivar was significantly higher than that of the other three cultivars (Fig. 1d).

Comprehensive analysis of primary fruit quality attributes among four apple cultivars

The total soluble solids (TSS) and total soluble sugar contents of the three mid-maturing cultivars—VG, RX, and RXH—were maintained at high levels, with all three exhibiting significantly higher values than the RFJ cultivar (Fig. 2a, b). Notably, the soluble pectin content in VG was significantly higher than that observed in RX, RXH, and RFJ (Fig. 2c). Regarding acidity profiles, the total acidity (TA) content of RX was significantly higher than that of all other cultivars, followed sequentially by RXH and RFJ, whereas VG exhibited the lowest TA accumulation (Fig. 2d). Furthermore, the TDF content of RX was significantly greater than that of VG, RXH, and RFJ (Fig. 2e). Conversely, the RFJ cultivar possessed a significantly higher total free amino acid content compared to the three mid-maturing varieties (Fig. 2f). Collectively, these findings demonstrate that VG, RX, and RXH exhibit superior overall fruit quality attributes under the unique low-latitude and high-altitude ecological conditions of the Zhaotong region. Moreover, each mid-maturing cultivar displays distinct advantages regarding specific functional nutritional components (such as dietary fiber and total sugars), thereby providing diversified, high-quality alternatives for optimizing the local apple varietal structure.

Profiling of nutritional and functional quality attributes among four apple cultivars

The nutritional and functional quality attributes of the four apple cultivars were systematically determined, and the results are illustrated in Fig. 3. The RXH cultivar exhibited significantly higher total phenolic and total anthocyanin contents compared to the other three groups (Fig. 3a, b). Conversely, the VG cultivar possessed significantly higher concentrations of vitamin C (VC) and vitamin E (VE) than the remaining three varieties (Fig. 3c, d). In terms of functional antioxidant capacity, the RXH cultivar displayed the highest ABTS radical scavenging activity, followed sequentially by RX and VG, while RFJ exhibited the lowest activity (Fig. 3e). A highly consistent trend was observed for DPPH radical scavenging activity, where RXH demonstrated the most potent capacity, followed by RX and VG, and RFJ presented the minimum efficacy (Fig. 3f). Collectively, these findings suggest that the antioxidant activities of these apple cultivars are strongly and positively correlated with their total phenolic and anthocyanin contents. Mid-maturing cultivars, particularly RXH, manifest outstanding antioxidant potential, which can likely be attributed to their elevated accumulation of polyphenols and flavonoids.

Evaluation of volatile and gustatory flavor profiles among four apple cultivars

The volatile and gustatory flavor characteristics of VG, RX, RXH, and RFJ apple cultivars were evaluated and compared utilizing electronic nose (e-nose) and electronic tongue (e-tongue) systems. Radar charts generated from the e-nose and e-tongue datasets revealed that the four apple cultivars shared a highly similar overall flavor skeleton, though distinct variations were observed in specific sensor response intensities. Regarding the volatile aroma profiles (Fig. 4a), all four cultivars elicited pronounced responses on the W1W (sulfides) and W5S (nitrogen oxides) sensors. Notably, the RX cultivar exhibited a significantly higher response intensity on the W1W sensor than the other cultivars, indicating a greater abundance of sulfide-based volatile organic compounds. This was followed sequentially by the RXH and RFJ cultivars, whereas the VG cultivar displayed the weakest overall aroma response intensity. Regarding the gustatory taste profiles (Fig. 4b), the taste wheels of the four cultivars demonstrated a high degree of overlap, with 'umami' and 'sweetness' constituting the core gustatory attributes across all samples. At a micro-analytical level, the RXH cultivar displayed a marginally higher sweetness response, whereas the RFJ cultivar exhibited slightly more intense responses for sourness and saltiness compared to the three mid-maturing cultivars. In conclusion, while the core gustatory dimensions of the four apple cultivars are highly conserved, their primary flavor variations reside in the emission intensities of volatile aroma compounds, particularly sulfide-like constituents.

Comparative metabolomic profiling and metabolic pathway analysis

To systematically resolve the chemical disparities among VG, RX, RXH, and RFJ apple cultivars, a comprehensive untargeted metabolomic analysis was performed. Principal component analysis (PCA) revealed distinct segregation profiles among the four cultivars,

https://doi.org/10.48130/frures-0026-0037

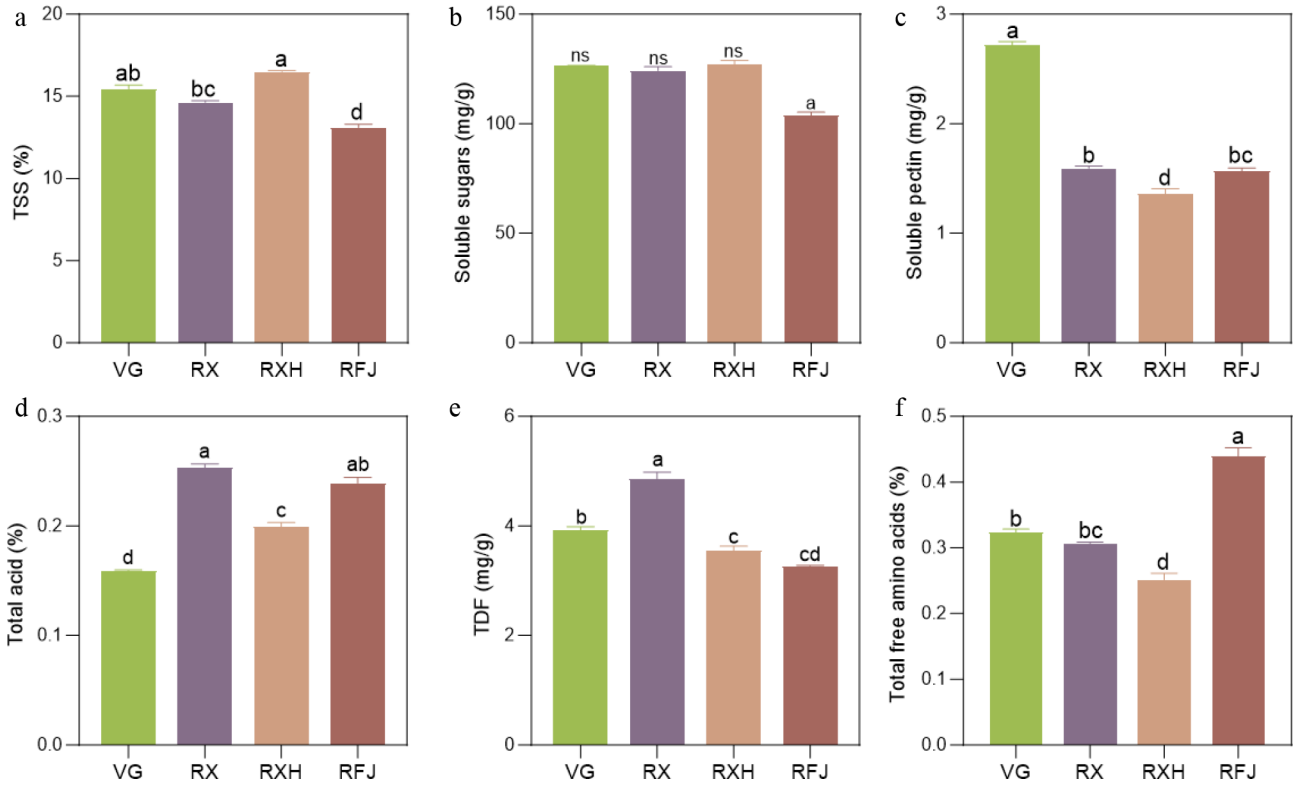


Fig. 2 Primary physicochemical and nutritional attributes among four apple cultivars. (a) Total soluble solids (TSS, %). (b) Total soluble sugars (mg/g FW). (c) Soluble pectin (mg/g FW). (d) Total titratable acidity (TA, % as malic acid equivalent). (e) Total dietary fiber (TDF, mg/g FW). (f) Total free amino acids (% FW). Data are presented as mean ± SEM (n = 5). Different lowercase letters indicate statistically significant differences among cultivars according to one-way ANOVA with Tukey's HSD test (p < 0.05).

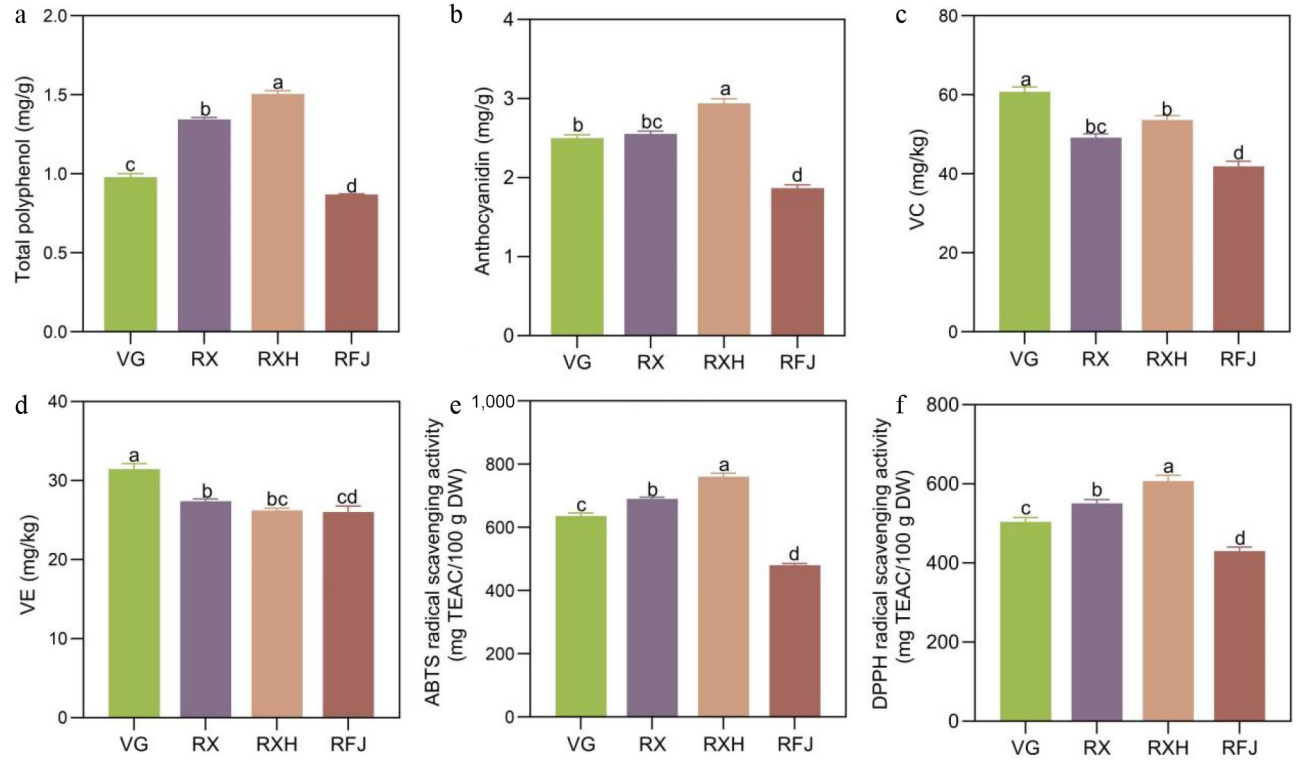


Fig. 3 Functional nutritional components and *in vitro* antioxidant activities among four apple cultivars. (a) Total phenolic content (TPC, mg/g FW). (b) Total anthocyanin content (TAC, mg/100 g FW). (c) Vitamin C (VC, mg/kg FW). (d) Vitamin E (VE, mg/kg FW). (e) ABTS radical scavenging activity (mg TEAC/100 g DW). (f) DPPH radical scavenging activity (mg TEAC/100 g DW). Data are expressed as mean ± SEM (n = 5). Different lowercase letters indicate statistically significant differences among cultivars according to one-way ANOVA with Tukey's HSD test (p < 0.05).

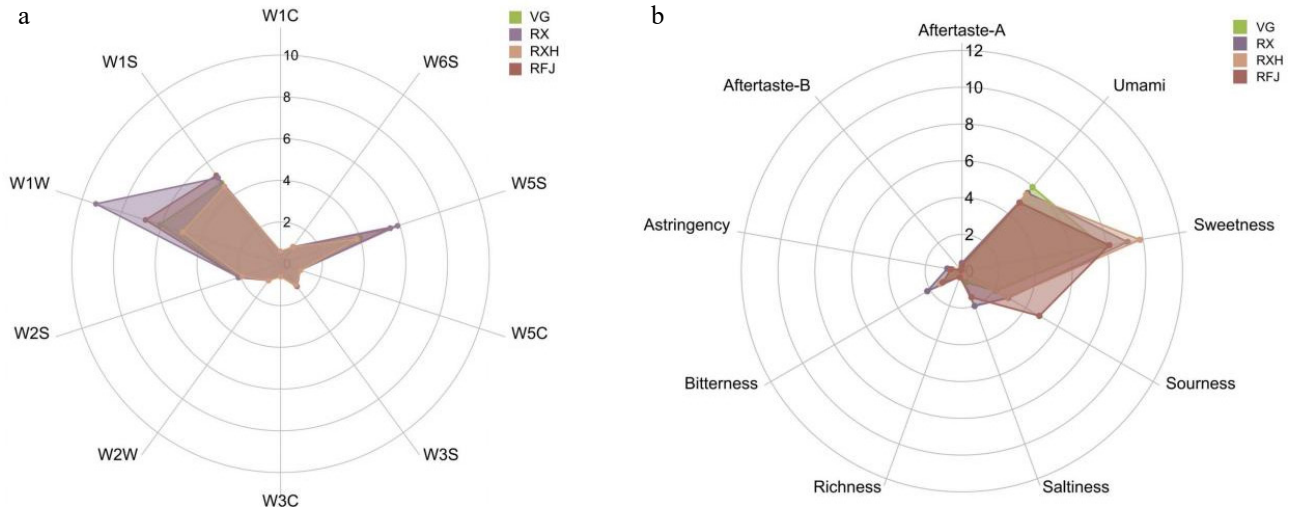


Fig. 4 Profiling of volatile and gustatory flavor characteristics among four apple cultivars. (a) Electronic tongue radar chart showing the gustatory taste profiles. (b) Electronic nose radar chart showing the volatile aroma sensor responses. Data are expressed as mean ± SEM (n = 5).

indicating that their global metabolic phenotypes are highly differentiated at the metabolite level (Fig. 5a). A hierarchical clustering heatmap of all differentially accumulated metabolites (DAMs) further illustrated their explicit abundance and accumulation patterns across the groups (Fig. 5b). Regarding metabolic pathway regulation, Kyoto Encyclopedia of Genes and Genomes (KEGG) enrichment analysis demonstrated that these metabolic alterations were predominantly driven by carbohydrate and amino acid metabolism Supplementary Table S1. Notably, the pentose phosphate pathway emerged as the most significantly enriched metabolic cascade, followed sequentially by glycolysis/gluconeogenesis and branched-chain amino acid biosynthesis (Fig. 5c). Furthermore, a network pathway-metabolite association map visually delineated the integration of core metabolic intermediates within these pathways (Fig. 5d). For instance, glucose 6-phosphate and fructose 6-phosphate were identified as shared key substrates simultaneously bridging glycolysis and the pentose phosphate pathway, while specific amino acids, such as isoleucine and L-arginine, played pivotal roles within their respective amino acid metabolic network.

Correlation analysis between fruit quality attributes and metabolomic profiles

To investigate the inner metabolic networks governing fruit quality, a correlation analysis was performed between primary fruit quality traits and differentially accumulated metabolites in Zhaotong apples (Fig. 6). As shown in the data associations presented in the heatmap, TSS and soluble sugars exhibited a co-varying directional pattern, whereas both indices displayed a marked inverse alignment with the data profiles of metabolites such as L-isoleucine, arginine, total free amino acids, 3-phosphoglyceric acid, and D-glucose 6-phosphate; concurrently, mutually consistent co-directional distributions were observed among these amino acid components and sugar phosphate intermediates, with pyridoxamine phosphate showing fluctuations that aligned with sugar-related indices yet deviated from free amino acids; in addition, the variation trend of total acid partially tracked those of TDF and soluble pectin, while gluconic acid and allantoic acid showed no pronounced regular patterns across the majority of the evaluated parameters.

Correlation analysis between electronic sensory attributes and metabolomic profiles

To elucidate the intrinsic linkages and regulatory networks bridging core metabolites and gustatory taste indicators, a correlation analysis was executed combining the electronic tongue sensory profiles and the differentially accumulated metabolite datasets of the four apple cultivars (Fig. 7). The correlation analysis revealed that free amino acids, including L-isoleucine and arginine, exhibited significant positive correlations with key carbohydrate metabolic intermediates, such as 3-phosphoglyceric acid and D-glucose 6-phosphate. Within the gustatory sensor matrices, positive correlations were observed among bitterness, astringency, and aftertaste attributes (Aftertaste-A and Aftertaste-B). Conversely, saltiness displayed a widespread and distinct negative correlation with the aforementioned primary free amino acids and glycolytic intermediates. Furthermore, D-fructose 6-phosphate and pyridoxamine phosphate manifested a pronounced negative correlation and antagonistic relationship with the majority of the aforementioned polysaccharide and amino acid metabolic indicators. In conclusion, these findings demonstrate that the overall gustatory flavor quality of Zhaotong apples (encompassing sourness, bitterness/astringency, and saltiness) is dynamically driven by the synergistic interactions and reciprocal flux variations between internal primary metabolites, particularly carbohydrates and free amino acids.

Discussion

In the field of apple fruit quality research, recent multi-dimensional advancements bridging phenotypic characteristics, nutritional values, flavor profiles, and metabolic regulation networks have provided vital frameworks for elucidating quality formation across different cultivars. Currently, global research on apple quality primarily centers on genetic background-driven phenotypic differentiation, the antioxidant efficacy of secondary metabolites, the construction of electronic sensory flavor wheels, and multi-omics-driven molecular regulatory mechanisms[8,16,31–33].

Studies have demonstrated that physical phenotypes and primary physicochemical indicators serve as the most straightforward determinants governing commercial value and market positioning[16]. Different plant lines exhibit variations in metabolic signaling; for

https://doi.org/10.48130/frures-0026-0037

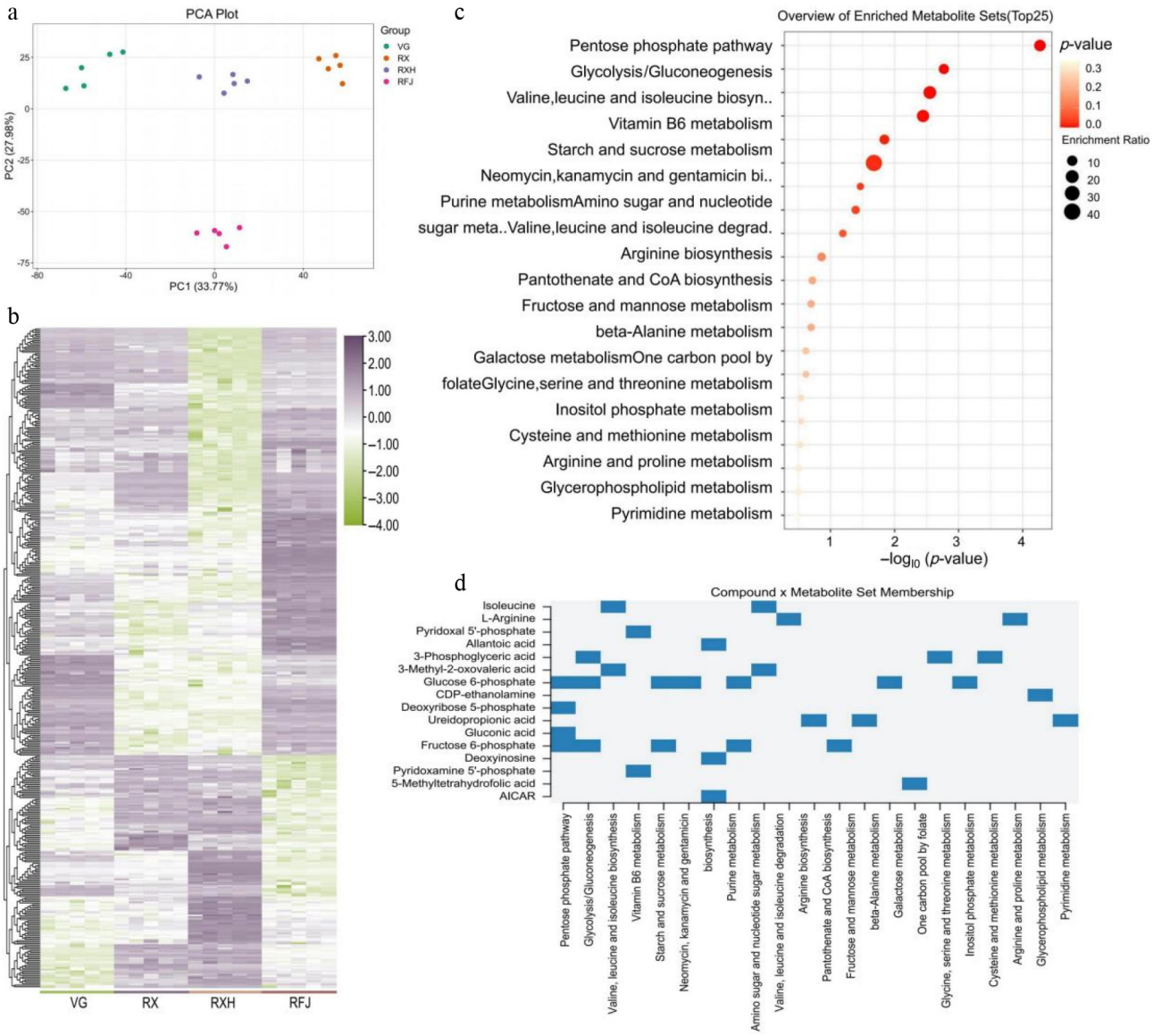


Fig. 5 Comparative untargeted metabolomic profiling and metabolic pathway enrichment among four apple cultivars. (a) Score scatter plot of principal component analysis (PCA) based on all identified metabolites in positive and negative ESI modes ($n = 5$). (b) Hierarchical cluster analysis (HCA) heatmap of differentially accumulated metabolites (DAMs; screening thresholds: VIP > 1.0, fold change ≥ 1.5 or ≤ 0.67, FDR-corrected $p < 0.05$). Columns represent biological replicates, and rows represent individual metabolites (Z-score standardized). (c) KEGG pathway enrichment bubble plot highlighting top-ranked metabolic pathways (p-values indicated by color gradient; enrichment ratio indicated by bubble diameter). (d) Network pathway-metabolite association matrix mapping key primary intermediates to enriched KEGG cascades.

example, different beet varieties typically show unique morphological characteristics and differences in sugar and acid accumulation under specific ecological niches[34]. Concurrently, with the expansion of health-conscious consumer demands, the 'composition-activity' synergistic networks of secondary and primary functional constituents—such as polyphenols, anthocyanins, flavonoids, and vitamins—have emerged as crucial research priorities, with polyphenols and anthocyanins frequently corroborated as the core contributors to *in vitro* antioxidant capacity in plants[5,35,36]. Regarding flavor perception, utilizing electronic nose (e-nose) and electronic tongue (e-tongue) systems to delineate fruit flavor evolution from both volatile and gustatory dimensions has become highly sophisticated[7,37]. Most investigations emphasize the structural overlap of core tastes (such as sweetness and umami) along with intensity variations in the release of specific volatile organic compounds, including sulfides, esters, and nitrogen oxides[38]. Furthermore, the introduction of untargeted metabolomics paired with correlation networks has yielded breakthroughs in linking macroscopic quality parameters to microscopic molecular pathways[39,40]. Specifically, the dynamic coordination and reciprocal flux shifts between carbohydrate metabolism (e.g., glycolysis and the pentose phosphate pathway) and amino acid metabolic networks are widely recognized as the fundamental mechanisms driving quality diversification during fruit development and ripening[41–43].

The findings of this study demonstrate that under the low-latitude and high-altitude ecological conditions of Zhaotong, the fruit diameter and single-fruit weight of the three mid-maturing cultivars—'Golden Venus' (VG), 'Ruixue' (RX), and 'Ruixianghong' (RXH)—exhibit a high degree of uniformity. Conversely, the transverse diameter and single-fruit weight of the traditional

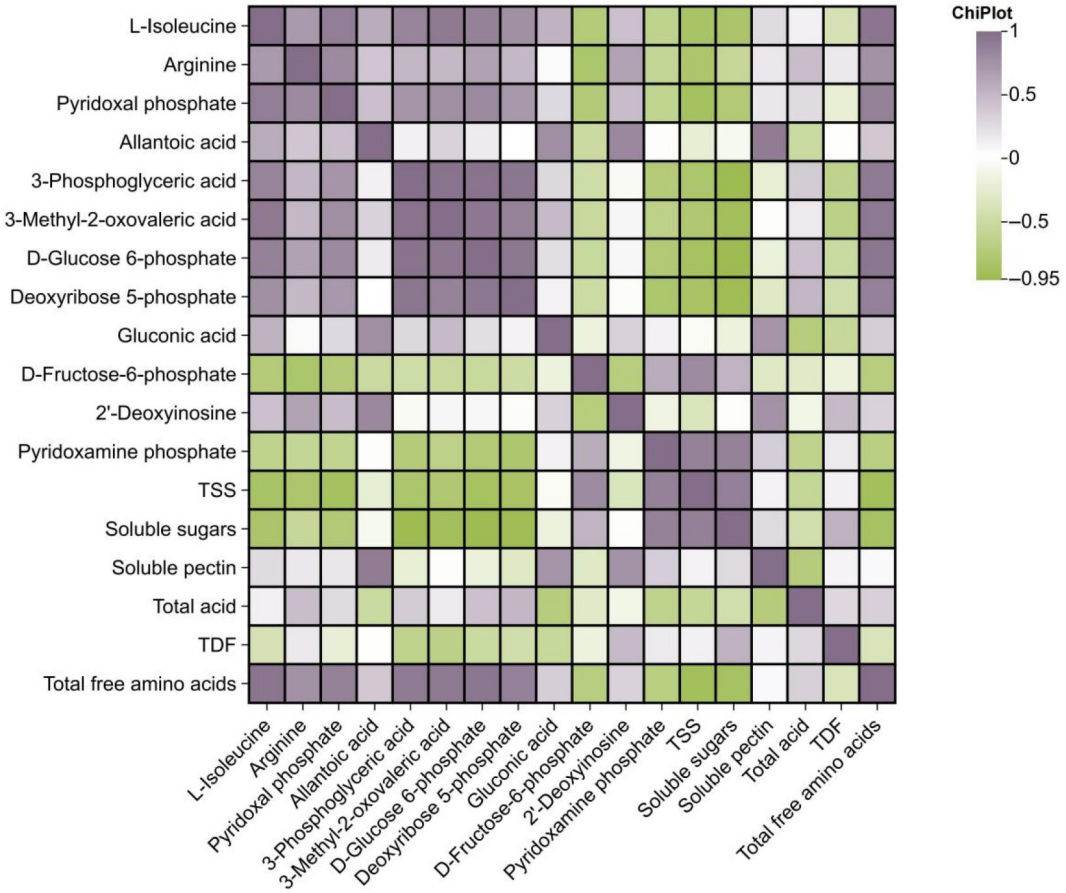


Fig. 6 Correlation matrix between primary quality traits and differentially accumulated metabolites (DAMs). Color scale corresponds to Pearson's correlation coefficients ($n = 5$). Significant correlations are established at $p < 0.05$.

late-maturing cultivar 'Red Fuji' (RFJ) are significantly greater than those of the mid-maturing cultivars, while its longitudinal diameter displays no statistically significant difference. This underscores that RFJ fruits within this ecological niche predominantly exhibit robust, lateral-development growth characteristics. Regarding primary physicochemical quality, the mid-maturing cultivars display a prominent 'high-sugar' attribute; their TSS and total soluble sugar contents are significantly superior to those of RFJ. This indicates that the intense sunlight and substantial diurnal temperature variations characteristic of the high-altitude Zhaotong region effectively stimulate carbohydrate assimilation and accumulation in mid-maturing cultivars. Nevertheless, the four apple cultivars exhibit distinct specificities in structural components and free amino acids: VG is highly enriched in soluble pectin, establishing the biochemical foundation for its unique flesh texture; RX possesses a significantly higher total acidity (TA) and TDF content, resulting in a more multi-layered sweet-and-sour flavor profile and higher nutritional value; and RFJ, despite its lower sugar accumulation, exhibits a significantly higher total free amino acid content compared to the mid-maturing varieties, thereby supplying the substrates for its gustatory diversity. In terms of nutrition and antioxidant capacity, the RXH cultivar possesses significantly higher total phenolic and total anthocyanin contents than the other three groups, coinciding with the highest ABTS and DPPH radical scavenging activities. This trend is strongly and positively correlated with polyphenol and anthocyanin concentrations, confirming that phenolic secondary metabolites are the core functional constituents driving the *in vitro* antioxidant potential of Zhaotong apples[30,44–46]. Additionally, VG displays the highest levels of vitamin C (VC) and vitamin E (VE), highlighting its excellent functional potential as a source of micronutrients.

From an electronic sensory perspective, the four apple cultivars share highly conserved volatile and gustatory flavor frameworks. E-nose profiling indicates that all samples elicit intense responses on the W1W (sulfides) and W5S (nitrogen oxides) sensors. Notably, the RX cultivar displays a significantly higher response value on the W1W sensor, suggesting an abundant accumulation of sulfide-like volatile compounds that contribute to its rich aroma profile, whereas VG exhibits the weakest overall volatile response. The e-tongue radar charts reveal a high degree of overlap in the taste profiles across all four cultivars, with 'umami' and 'sweetness' acting as the absolute dominant core attributes. At a micro-analytical level, RXH displays a marginally higher sweetness response, which aligns with its high-sugar and low-acid sensory experience. Concurrently, the slightly stronger responses of RFJ to sourness and saltiness indices reflect its unique flavor coordination effects.

Untargeted metabolomic analysis further verifies that the four apple cultivars achieve distinct and clear phenotypic segregation across global metabolite profiles, with core metabolic alterations predominantly clustered within carbohydrate and amino acid pathways. Among all differentially regulated pathways, the pentose phosphate pathway (PPP) and glycolysis/gluconeogenesis are the most significantly enriched. As shared key intermediates, the flux and abundance variations of glucose-6-phosphate and fructose-6-phosphate directly modulate primary quality traits across different cultivars. Meanwhile, the enrichment of differential metabolites

https://doi.org/10.48130/frures-0026-0037

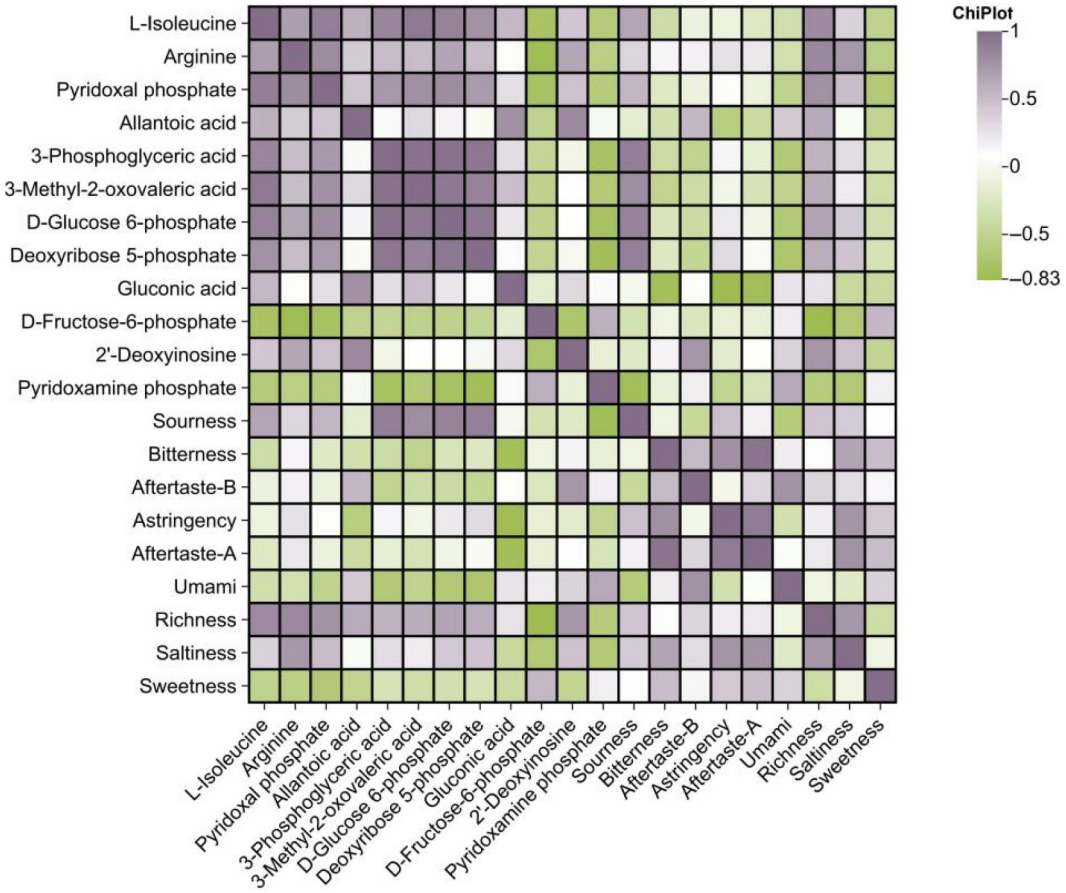


Fig. 7 Correlation matrix between electronic sensory attributes (electronic tongue) and core metabolites. Color intensity illustrates Pearson's correlation coefficients ($n = 5$). Significant correlations are established at $p < 0.05$.

such as isoleucine and L-arginine within the branched-chain amino acid and arginine metabolic pathways directly participates in regulating free amino acid pools.

Multidimensional correlation analysis provides a deeper elucidation of the 'carbon-nitrogen balance and electronic sensory regulatory network' that governs fruit ripening and flavor development. The correlation datasets reveal that free amino acids, including L-isoleucine and arginine, are significantly and positively correlated with carbohydrate metabolic intermediates such as 3-phosphoglyceric acid, indicating a high degree of intrinsic synergy between carbon and nitrogen source supplies during primary metabolism. However, the final quality indices (TSS and soluble sugars) display prominent and statistically significant negative correlations with these primary free amino acids as well as the total free amino acid pool. This trade-off reveals that during fruit development and ripening, Zhaotong apples actively initiate amino acid transformation and consumption to maintain high-level accumulation of soluble carbohydrates and TSS. Furthermore, correlation analysis integrating electronic sensory profiles with differential metabolite matrices indicated that electronic-tongue sourness scores were significantly associated with key glycolytic intermediates (3-phosphoglyceric acid and glucose 6-phosphate), whereas fructose 6-phosphate and pyridoxamine phosphate exhibited pronounced potential correlations with the majority of polysaccharide and amino acid indices.

This uncovers a biochemical network governing sugar-acid co-metabolism in apples at the molecular level, which aligns closely with previously reported associations between the tricarboxylic acid (TCA) cycle and carboxylic acid metabolic networks. Additionally, the negative correspondence of saltiness scores with major free amino acids and carbohydrate intermediates echoes previous findings regarding how distinct metabolite profiles modulate human taste-neural processing[47–49]. Simultaneously, the positive correlation linkage among bitterness, astringency, and aftertaste (Aftertaste-A and Aftertaste-B) indicates a coexistence and synergistic interplay among internal flavor-active compounds dominated by polyphenols or specific amino acids. In conclusion, the essential disparities among the four cultivars are dynamically driven by the synergistic interactions and reciprocal flux variations within primary metabolic networks, particularly carbohydrate and free amino acid pathways.

Conclusions

In conclusion, this study demonstrates that under the low-latitude and high-altitude ecological conditions of the Zhaotong region, the three introduced mid-maturing apple cultivars—VG, RX, and RXH—exhibit distinct physicochemical quality attributes and prominent functional nutritional profiles compared to the traditional late-maturing RFJ. Notably, RXH showed remarkable polyphenol accumulation and antioxidant potential, whereas VG was characterized by superior vitamin levels. Furthermore, the multidimensional differentiation in flavor profiles (encompassing electronic tongue sensor responses and characteristic volatile features) across the four cultivars is closely associated with divergent patterns in primary metabolic networks, particularly involving carbohydrate

metabolism (glycolysis and related sugar transformations) and free amino acid pathways. Overall, these findings elucidate the characteristic phenotypic, sensory, and metabolic signatures of Zhaotong specialty apples, establishing an objective empirical basis and scientific framework for regional germplasm evaluation, cultivar optimization, and precise postharvest utilization.

Author contributions

The authors confirm their contributions to the paper as follows: original draft preparation, analysis and interpretation of results: Li X; data collection: Li X, Xiang Y, Li Y; draft manuscript preparation: Zhang M, Liu K, Ma X; financial support: Zhang M, Ma X. All authors reviewed the results and approved the final version of the manuscript.

Data availability

The raw data supporting the conclusions of this article will be made available by the authors, without undue reservation.

Acknowledgments

This study was supported by the Scientific Research Startup Fund of Southwest Forestry University (Grant No. 110225092/01102), the National Natural Science Foundation of China (Grant No. 82560646), the Science and Technology Special Project of Yunnan Universities Serving Key Industries (Grant No. 2025-251), and the Special Fund for Yongsheng County Academician-Farmer Science and Technology Service Station (Grant No. Yuncaijiao [2024]-18).

Conflict of interest

The authors declare that they have no conflict of interest.

Supplementary information accompanies this paper online at: https://doi.org/10.48130/frures-0026-0037.

Dates

Received 21 July 2026; Revised 8 September 2026; Accepted 21 September 2026; Published online 13 October 2026

References

[1] Cornille A, Giraud T, Smulders MJM, Roldán-Ruiz I, Gladieux P. 2014. The domestication and evolutionary ecology of apples. *Trends in Genetics* 30:57–65

[2] Ke B, Zhang Q. 2024. Assessing the efficiency and potential of China's apple exports. *Complexity* 2024:7816792

[3] Lu J, Song W, Zuo X, Zhu D, Wei Q. 2023. A study of apple orchards extraction in the Zhaotong Region based on sentinel images and improved spectral angle features. *Applied Sciences* 13:11194

[4] Kim K, Park M, Kwon D, Wang Y, Sung J. 2025. Antioxidant and flavor properties of different apple cultivars grown in Korea. *Food Chemistry: X* 32:103263

[5] Hyson DA. 2011. A comprehensive review of apples and apple components and their relationship to human health. *Advances in Nutrition* 2:408–420

[6] Qu R, Chen J, Li W, Jin S, Jones GD, et al. 2023. Consumers' preferences for apple production attributes: results of a choice experiment. *Foods* 12:1917

[7] Lu L, Hu Z, Hu X, Li D, Tian S. 2022. Electronic tongue and electronic nose for food quality and safety. *Food Research International* 162:112214

[8] Tan J, Xu J. 2020. Applications of electronic nose (e-nose) and electronic tongue (e-tongue) in food quality-related properties determination: a review. *Artificial Intelligence in Agriculture* 4:104–115

[9] Fiehn O. 2016. Metabolomics by gas chromatography–mass spectrometry: combined targeted and untargeted profiling. *Current Protocols in Molecular Biology* 114:1–32

[10] Zhang Y, Zhang H, Wang X, Liu Y, Zhang Y, et al. 2026. Comprehensive widely targeted metabolomics and transcriptomics analysis revealed the key differential genes and metabolites underlying the formation of taste tomato quality. *Food Quality and Safety* 10:fyag003

[11] Ma Y, Devi MJ, Song L, Gao H, Jin L, et al. 2024. Multi-omics integration analysis reveals metabolic regulation of carbohydrate and secondary metabolites during goji berry (*Lycium barbarum* L.) maturation. *Postharvest Biology and Technology* 218:113184

[12] Li D, Min Y, Cheng C, Liu X, Xie X, et al. 2025. The diversity and disparity of mineral elements in global kiwifruits. *Food Research International* 203:115844

[13] Sampaio M, Rocha M, Dias O. 2024. A multi-omics approach for understanding grape metabolism throughout development. *IFAC-PapersOnLine* 58:43–48

[14] Zhang H, Zhang C, Ni Z, Yue Q, Li Z, et al. 2025. Uncovering key flavor-related pathways in mango cultivars from Yunnan by integrated transcriptomics and metabolomics analyses. *Food Bioscience* 69:106870

[15] Li W, Wan A, Li J, Chen K, Ma Z, et al. 2025. A review of data-driven key technologies for intelligent citrus systems. *Computers and Electronics in Agriculture* 239:111121

[16] Musacchi S, Serra S. 2018. Apple fruit quality: overview on pre-harvest factors. *Scientia Horticulturae* 234:409–430

[17] Ma C, Sun Z, Chen C, Zhang L, Zhu S. 2014. Simultaneous separation and determination of fructose, sorbitol, glucose and sucrose in fruits by HPLC–ELSD. *Food Chemistry* 145:784–788

[18] Aprea E, Corollaro ML, Betta E, Endrizzi I, Demattè ML, et al. 2012. Sensory and instrumental profiling of 18 apple cultivars to investigate the relation between perceived quality and odour and flavour. *Food Research International* 49:677–686

[19] Figuerola F, Hurtado ML, Estévez AM, Chiffelle I, Asenjo F. 2005. Fibre concentrates from apple pomace and citrus peel as potential fibre sources for food enrichment. *Food Chemistry* 91:395–401

[20] Chen H, Cao S, Fang X, Mu H, Yang H, et al. 2015. Changes in fruit firmness, cell wall composition and cell wall degrading enzymes in postharvest blueberries during storage. *Scientia Horticulturae* 188:44–48

[21] Singleton VL, Orthofer R, Lamuela-Raventós RM. 1999. Analysis of total phenols and other oxidation substrates and antioxidants by means of folin-ciocalteu reagent. In *Methods in Enzymology*. Amsterdam: Elsevier. pp. 152–178 doi: 10.1016/s0076-6879(99)99017-1

[22] Wolfe K, Wu X, Liu RH. 2003. Antioxidant activity of apple peels. *Journal of Agricultural and Food Chemistry* 51:609–614

[23] Tsao R, Yang R, Xie S, Sockovie E, Khanizadeh S. 2005. Which polyphenolic compounds contribute to the total antioxidant activities of apple? *Journal of Agricultural and Food Chemistry* 53:4989–4995

[24] Kevers C, Falkowski M, Tabart J, Defraigne JO, Dommes J, et al. 2007. Evolution of antioxidant capacity during storage of selected fruits and vegetables. *Journal of Agricultural and Food Chemistry* 55:8596–8603

[25] Chun J, Lee J, Ye L, Exler J, Eitenmiller RR. 2006. Tocopherol and tocotrienol contents of raw and processed fruits and vegetables in the United States diet. *Journal of Food Composition and Analysis* 19:196–204

[26] Conforti PA, Patrignani M. 2025. Antioxidant activity from non-conventional beverage plant sources in Argentina. *Beverage Plant Research* 5:e006

[27] Weerabaddhanage AM, Pavalakumar D, Edirisingha IP, Gunathunga CJ, Thivijan S, et al. 2025. Characterization of probiotic and antioxidant properties in Saccharomyces and non-Saccharomyces yeasts isolated from Sri Lankan grape wine fermentation. *Studies in Fungi* 10:e020

https://doi.org/10.48130/frures-0026-0037

[28] Xie J, Wang Q, Cui H, Wang L, Deng Y, et al. 2024. Characterization of Gardenia tea based on aroma profiles using GC-E-Nose, GC-O-MS and GC × GC-TOFMS combined with chemometrics. *Beverage Plant Research* 4:e001

[29] Fan X, Pan L, Chen R. 2023. Characterization of flavor frame in grape wines detected by HS-SPME-GC-MS coupled with HPLC, electronic nose, and electronic tongue. *Food Materials Research* 3:9

[30] Wojdyło A, Oszmiański J, Laskowski P. 2008. Polyphenolic Compounds and Antioxidant Activity of New and Old Apple Varieties. *Journal of Agricultural and Food Chemistry* 56:6520−6530

[31] Shi H, Guo T, Wei C, Tian J, Hou X, et al. 2025. Integrative multi-omics reveals quality markers and metabolic pathways across genotype and ripening gradients in high-altitude *Malus*. *Foods* 14:4039

[32] Duan N, Bai Y, Sun H, Wang N, Ma Y, et al. 2017. Genome re-sequencing reveals the history of apple and supports a two-stage model for fruit enlargement. *Nature Communications* 8:249

[33] Corollaro ML, Aprea E, Endrizzi I, Betta E, Demattè ML, et al. 2014. A combined sensory-instrumental tool for apple quality evaluation. *Postharvest Biology and Technology* 96:135−144

[34] Hassani M, Mahmoudi SB, Saremirad A, Taleghani D. 2023. Genotype by environment and genotype by yield*trait interactions in sugar beet: analyzing yield stability and determining key traits association. *Scientific Reports* 13:23111

[35] Kschonsek J, Wolfram T, Stöckl A, Böhm V. 2018. Polyphenolic compounds analysis of old and new apple cultivars and contribution of polyphenolic profile to the in vitro antioxidant capacity. *Antioxidants* 7:20

[36] Lu Z, Wang X, Lin X, Mostafa S, Zou H, et al. 2024. Plant anthocyanins: classification, biosynthesis, regulation, bioactivity, and health benefits. *Plant Physiology and Biochemistry* 217:109268

[37] Munekata PES, Finardi S, de Souza CK, Meinert C, Pateiro M, et al. 2023. Applications of electronic nose, electronic eye and electronic tongue in quality, safety and shelf life of meat and meat products: a review. *Sensors* 23:672

[38] Al Shoffe Y, Rudell D, Park D, Algul BE, Qin M, et al. 2024. Aroma volatiles and sensory quality of organically-grown apple cultivars after dynamic controlled atmosphere (DCA) storage and comparison with CA-stored fruit with and without 1-methylcyclopropene (1-MCP). *Postharvest Biology and Technology* 218:113162

[39] Putri SP, Ikram MMM, Sato A, Dahlan HA, Rahmawati D, et al. 2022. Application of gas chromatography-mass spectrometry-based metabolomics in food science and technology. *Journal of Bioscience and Bioengineering* 133:425−435

[40] Lai R, Shen C, Feng X, Gao M, Zhang Y, et al. 2022. Integrated metabolomic and transcriptomic analysis reveals differential flavonoid accumulation and its underlying mechanism in fruits of distinct *Canarium album* cultivars. *Foods* 11:2527

[41] Fernie AR, Schauer N. 2009. Metabolomics-assisted breeding: a viable option for crop improvement? *Trends in Genetics* 25:39−48

[42] Zhang Y, Li P, Cheng L. 2010. Developmental changes of carbohydrates, organic acids, amino acids, and phenolic compounds in 'Honeycrisp' apple flesh. *Food Chemistry* 123:1013−1018

[43] Davey MW, Van Montagu M, Inzé D, Sanmartin M, Kanellis A, et al. 2000. Plant L-ascorbic acid: chemistry, function, metabolism, bioavailability and effects of processing. *Journal of the Science of Food and Agriculture* 80:825−860

[44] Boyer J, Liu RH. 2004. Apple phytochemicals and their health benefits. *Nutrition Journal* 3:5

[45] Chun OK, Kim DO, Smith N, Schroeder D, Han JT, et al. 2005. Daily consumption of phenolics and total antioxidant capacity from fruit and vegetables in the American diet. *Journal of the Science of Food and Agriculture* 85:1715−1724

[46] Sadilova E, Carle R, Stintzing FC. 2007. Thermal degradation of anthocyanins and its impact on color and *in vitro* antioxidant capacity. *Molecular Nutrition & Food Research* 51:1461−1471

[47] Sweetlove LJ, Beard KFM, Nunes-Nesi A, Fernie AR, Ratcliffe RG. 2010. Not just a circle: flux modes in the plant TCA cycle. *Trends in Plant Science* 15:462−470

[48] Keast RSJ, Breslin PAS. 2003. An overview of binary taste–taste interactions. *Food Quality and Preference* 14:111−124

[49] Fernie AR, Carrari F, Sweetlove LJ. 2004. Respiratory metabolism: glycolysis, the TCA cycle and mitochondrial electron transport. *Current Opinion in Plant Biology* 73:254−261

Copyright: © 2026 by the author(s). Published by Maximum Academic Press, Fayetteville, GA. This article is an open access article distributed under Creative Commons Attribution License (CC BY 4.0), visit https://creativecommons.org/licenses/by/4.0/.